Catalysis Letters 8 (1991) 67–100

APPLICATIONS OF POSITRON TECHNIQUES TO SURFACE STUDIES AND CATALYSIS

J. LAHTINEN and A. VEHANEN *

Laboratory of Physics, Helsinki University of Technology, 02150 Espoo, Finland

Received 10 July 1990; accepted 7 October 1990

Positron, positronium, surfaces, catalysis

Positrons can be used to obtain unique information on solids. The life and annihilation of this anti-matter particle is extremely sensitive to the atomic and electronic environment. Studies of solid surfaces with monoenergetic positron beams have found increasingly interesting applications and many new techniques have been introduced with unique results. The more traditional techniques using polyenergetic positrons have been utilized in the study of internal surfaces closely related to catalysis. In this review different positron techniques are described and their applications in the field of surface science and catalysis are presented.

1. Introduction

Positron, the anti-particle for electron, was first detected by Anderson in 1933 [1] shortly after the predictions of Dirac. Since that a great body of research has been done concerning the nature of this particle. The knowledge has first been applied to the fields of nuclear and elementary particle physics and then also to fields like medical research, chemistry and solid state physics [2].

Positrons are produced either in radioactive isotopes by nuclear reaction or by pair production using energetic electromagnetic radiation. The energy spectra in both cases are continuous ranging up to MeV range. The generation of monoenergetic positron beams also utilizes these positron sources but an energy conversion process is performed at the initial stage of beam formation.

In solid state physics positrons can be used either as polyenergetic positrons or as a monoenergetic beam. The broad energy spectrum of positrons emitted from a radioactive β^+ source is utilized in conventional positron spectroscopies. With different types of measurements information on open-volume defects inside the bulk can obtained [3,4]. The techniques are based on the trapping of positrons into areas where the atomic density is low, e.g. in vacancies or internal voids.

* Present address: Outokumpu Invest, P.O. Box 280, 00101 Helsinki, Finland

These methods are currently standard tools in the field of materials research for studies on e.g. properties of lattice defects.

The use of positron annihilation to study catalytic materials has been quite modest, although the technique can be regarded as an in-situ method to study internal surfaces. Once positrons have been implanted inside a porous material, information on the chemical environment is carried by γ-quanta emitted in the annihilation process. The position is sensitive to changes caused by metal deposition, by adsorption or by formation of chemical compounds on the internal surfaces, processes that are of great interest in catalysis research. Positron annihilation spectroscopy has been introduced as a potential tool for catalysis research [5].

Monoenergetic positron beams have become a powerful probe for solid surface and near-surface phenomena [4,6]. Various positron spectroscopies yield complementary information to their electron counterparts, while positron localization into open-volume defects provides unique possibilities to detect disorder in the near-surface region. Studying defects with monoenergetic positron beams was one of the first two applications of this technique and has remained a very important research area [7]. With variable energy positron beams the spatial defect distributions can be measured by changing the implantation energy and thus the mean implantation depth of the positrons.

Recent positron beam experiments have shown that positrons are highly sensitive to adsorbed surface atoms and molecules. A complementary technique to many electron spectroscopies has been developed. Low energy positron diffraction was observed by Rosenberg et al. [8]. Positron induced Auger electron spectroscopy (PAES) [19] is sensitive only to the topmost atomic layer because the process can take place only when the positron is localized at a surface state outside the metal bulk as can be seen in fig. 1. The surface sensitivity of PAES and the signal to noise ratio is superior to that of conventional AES. Positron

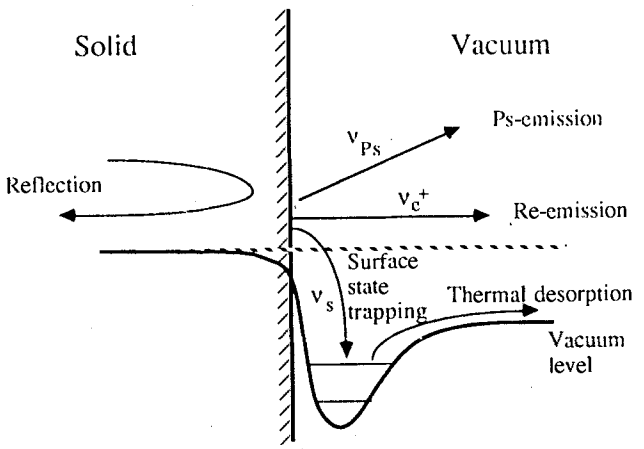

Fig. 1. Schematic picture of thermal positron-surface interaction mechanisms shown for a negative work function surface [10].

microscopes [11] and positron re-emission microscopes [12] can be used in a similar way to electron microscopes. These techniques can give information on the surface due to the unique properties of positrons and on the absence of the exchange interaction.

Reviews about applications of positrons have been written from different viewpoints by several authors: Schultz and Lynn [6] have given a review of positron beams and discussed the interaction of positrons with solids. Vehanen [7] has reviewed the applications of positron beam technique to study point defect distributions near the solid surface, and Tandberg et al. [13] have reviewed defect profiling of semiconductor epilayers. Cheng et al. [5] have given a review of the applications of polyenergetic positrons to study catalytic materials. Positron interactions with solid is also the topic of the books edited by Hautojärvi [3] and by Brandt and Dupasquier [4]. Positron and positronium chemistry has recently been reviewed in the book edited by Schrader and Jean [14]. In addition to the reviews the proceedings of the International Conferences on Positron Annihilation [15–17] should be mentioned here.

This paper reviews the surface science studies made with the low-energy positron technique and research applications to catalyst materials where the positron lifetime technique has normally been utilized. Section 2 discusses positron interactions with solid materials and section 3 describes the different experimental techniques. Section 4 deals with applications of monoenergetic positron beams to surface and near-surface studies. Section 5 describes the work done in catalytic systems and section 6 concludes the paper.

2. Positron interaction with solids and surfaces

The main difference in the interaction of positrons with solid surfaces when compared to electrons is associated with the opposite charge. There is also a difference due to the face that there is no Fermi sea of positrons in the sample and therefore the exchange interaction is absent. Due to the short positron lifetimes there is normally only one positron at a time inside the sample. For these reasons much of what has been studied with positrons complements other work and provides unique insight into the fundamental interactions of charged particles with matter. Some of the most important processes of positron interactions with solid surfaces are schematically illustrated in fig. 2. The figure is divided into four sequential time scales, each illustrating features that are appropriate to the frame. The different processes are described below according to the time sequence [6].

2.1. ENTRANCE AND SLOWING DOWN

A positron approaching the solid surface can either scatter from the surface potential or penetrate into the material. Scattering from the surface can be either

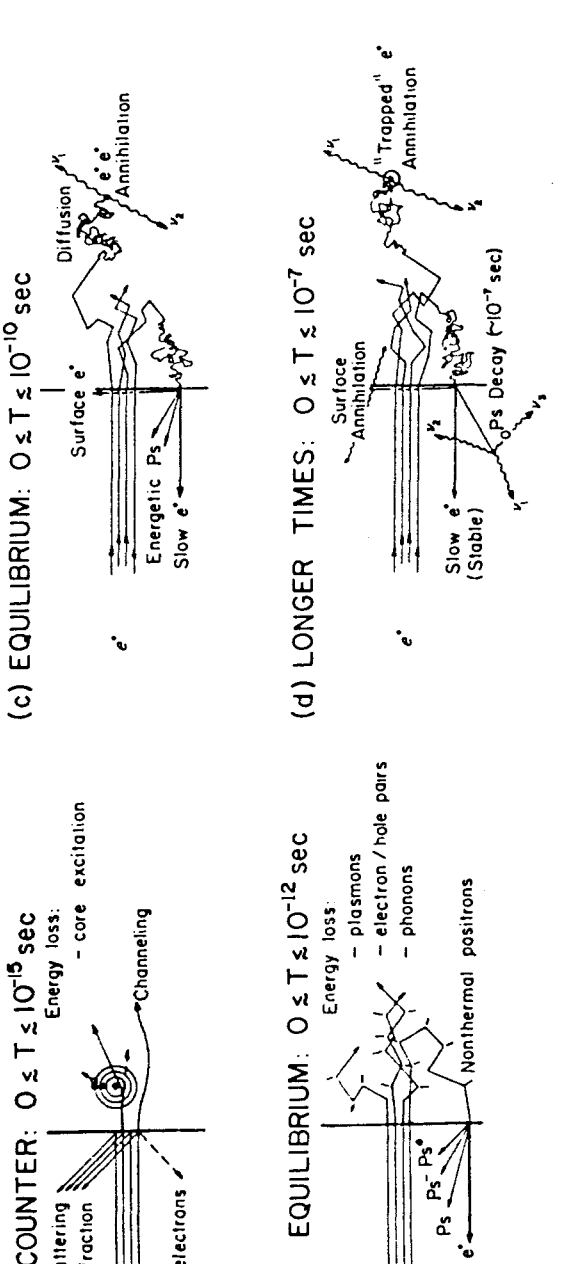

Fig. 2. Positron interaction with solid material. The figure is organized according to the time scales of positron slowing-down processes. Incident positrons will either scatter from the surface or penetrate into the material. Thermal equilibrium is achieved in about 1 ps. Thermalized positrons diffuse in the material and annihilate with free electrons or become localized in open volume defects. Thermalized positrons can also diffuse back to the surface and a spontaneous re-emission can occur if the positron work function is negative. Positrons may also be emitted from the solid as positronium atoms (Ps). Positrons or positronium can also be emitted from the sample before thermalization or they can annihilate during the slowing-down process [6].

elastic or inelastic. The former is utilized in low energy positron diffraction [8]. When the positron kinetic energy becomes large (several keV) the surface processes become relatively unimportant.

In the case of monoenergetic positrons implanted into the sample the depth distribution has the shape of a derivative of a Gaussian function. The mean implantation depth, $\bar{z}$, depends on the implantation energy E according to a power law

$$\bar{z} = A \cdot E^{1.6}, \tag{1}$$

where A equals 4.0 $\mu g/cm^2$ and E is given in keV [18,19]. From this equation implantation depths ranging from zero up to 50 μm range can be obtained. The controlled implantation depth has been utilized in the studies of near-surface defect distributions [7].

When positrons coming directly from a radioactive source are used the effect of the entrance surface is negligible. Positrons are implanted into the material with a mean penetration depth varying up to a few hundreds of μm depending on the β^+ source and sample density.

Positrons loose a major part of their energy by ionizing the material in a time scale of 10^{-13} s after implantation [20]. Thermal equilibrium is achieved in 10^{-12} s by plasmon, electron-hole pair and phonon excitations listed with decreasing energy. Positrons can also escape from the sample before complete thermalization or they can annihilate during the slowing-down process.

2.2. DIFFUSION AND TRAPPING

After positrons are thermalized they execute a diffusive motion in the material. In a perfect metal single crystal all positrons annihilate as free particles from a Bloch-like state with a lifetime between 100 and 200 ps [3]. The positron diffusion is governed by scattering from acoustic phonons [21], and the distance traveled inside the sample can be estimated from the lifetime and the diffusion coefficient, and is of the order of 1000 Å.

A positron diffusing inside the bulk has a relatively high probability of being localized into an open volume defect, because defect sites, where one or several positively charged atoms are missing, form an attractive potential minimum for positrons. Lifetimes of the localized positrons are between 200 and 500 ps and the lifetimes as well as the energies of the annihilation quanta vary with the type of the defect and give information on the electronic structure in the defect [3].

Positrons surviving annihilation and trapping processes inside the sample can diffuse back to the entrance surface. The potential that positrons experience at the surface is depicted in fig. 1. The potential minimum formed by the image potential can be used to trap positrons outside the surface. Annihilation of these positrons is extremely sensitive to the electronic environment at the surface and

this feature has been used e.g. in positron annihilation induced Auger electron spectroscopy [9].

2.3. EMISSION PROCESSES

Like the electron work function ϕ_- the positron work function ϕ_+ is defined as the minimum energy required to remove a positron from the bulk to the vacuum. The work function is a sum of the chemical potential and the surface dipole. The chemical potential consists of two components: repulsion by the ion cores and attraction by the electrons. The surface dipole, primarily caused by the tail of the electron distribution extending into the vacuum, prevents electron from escaping into the vacuum but attracts positrons at the surface.

The values for ϕ_+ are very close to zero and for several surfaces also negative giving rise to a spontaneous emission of positrons. The experimental values for negative ϕ_+ vary from -3.0 eV for W(110) to -0.05 eV for Al(100) [22]. The positron emission has narrow angular and energy spreads, which are utilized in the generation of slow positron beams.

Positrons may also be emitted from the solid as a positronium atom (Ps), which is the bound state between an electron and a positron [23]. The emission of Ps has wide energy and angular spreads and the maximum kinetic energy is

$$E_{ps} = -\phi_+ - \phi_- + 6.8 \text{ eV}, \tag{2}$$

where the value 6.8 eV is the Ps atom binding energy which is large enough to ensure negative E_{ps} values in most materials. There is no evidence of Ps formation inside the undefected bulk of metals or semiconductors, but there is a finite probability that Ps is formed when a positron leaving the surface travels through the decreasing electron density just outside the surface. In insulators Ps formation can occur also inside the bulk [23].

Positronium can exist in two different states. The para-positronium (p-Ps) or singlet state ($^1S_0$) has a lifetime of 125 ps in vacuum and annihilates by emitting two γ quanta. The triplet state ($^3S_1$) or ortho-positronium (o-Ps) has a lifetime of about 142 ns in vacuum and it decays by emitting three γ quanta. The o-Ps lifetime can be shortened by pick-off annihilation, where the o-Ps atom interacts with an external electron with opposite spin, resulting in rapid annihilation. The o-Ps lifetime and pick-off annihilation have been used to extract information on the internal surfaces of supported catalysts with and without additional species on the surfaces, as discussed in section 5.

In summary, positrons coming from inner parts of the material to the surface can be emitted out from the solid as thermal positrons, be trapped at the surface state or form positronium atoms that are ejected out. These phenomena are sensitive functions of surface conditions, e.g. sample temperature, presence of adsorbates, surface defects and surface orientation. When monoenergetic positrons are used the entrance surface can be examined with different techniques de-

scribed in section 4. When high specific surface area samples are studied the continuous energy spectrum of positron sources are utilized and positrons are implanted at various depths inside the sample. In that case most of the positrons take part in the surface processes at the internal surfaces.

3. Experimental techniques

3.1. POSITRON SOURCES

Positrons are obtained in two ways: from the decay of neutron-deficient β^+ radio-isotopes and from $e^- - e^\pm$ pair production of high energy γ-rays. For most applications the radioisotope decay is the most convenient way to produce positrons.

In β^+ sources a nuclear γ is emitted when the nucleus returns to its ground state a few picoseconds after e^+ emission. This γ can be used to give an indication of positron emission from the nucleus. The ^{22}Na-isotope is most commonly used in the experiments because of the relatively long half-life of 2.7 years. The other common isotope is ^{58}Co, but due to the much shorter half-life of 71 days this source is used in more special cases, e.g. in an UHV environment, where the use of Na is more difficult [24]. The continuous energy spectrum of positrons emitted from the ^{58}Co source is shown in fig. 3.

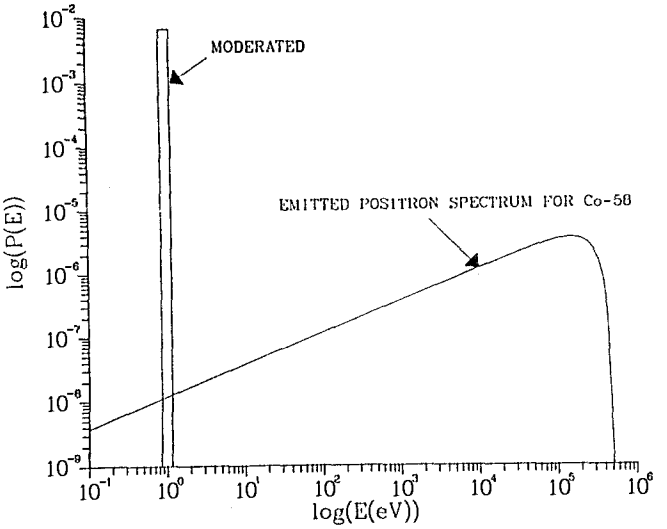

Fig. 3. Energy spectra from a radioactive ^{58}Co source before and after the moderation process [6]. Although most of the positrons are lost in the moderation process the brightness i.e. number of positrons in energy interval, has increased more than three decades.

The e^-–e^+ pair production can be used when a LINAC is available [25]. In this case the pulsed electron beam is stopped in a high-Z material creating bremsstrahlung γ-rays which then form electrons and positrons. With this kind of positron source the intensity of the source can easily be varied.

3.2. MEASURED QUANTITIES

In positron experiments several parameters can be measured. The measured signals based on the annihilation radiation are the positron lifetime, the annihilation line shape, the angular correlation spectrum of γ-rays or the amount of positronium. In addition to the annihilation radiation positrons themselves can be detected, and in some cases also secondary electrons, characteristic X-rays, UV-photons or Ps atoms have been measured directly.

The most widely used signal is the positron lifetime that is obtained from the time difference between nuclear (start) and annihilation (stop) γ's. A schematic diagram of a typical positron lifetime apparatus is shown in fig. 4. It utilizes two plastic scintillators connected to fast electronics capable of measuring the time difference averaging from 100 ps to 140 ns between the two events. The time differences are sorted and collected with a multichannel analyzer. A lifetime spectrum is obtained as a result, from which the average lifetime and various lifetime components can be calculated [3].

In Angular Correlation of Annihilation Radiation (ACAR) the angular distribution of annihilation photons is measured. The photon momentum distribution reflects the electron density of states and thus the electron momentum distribution can be calculated from the measured signal [3]. The ACAR spectra are measured using two detectors on opposite sides of the sample by rotating one of the detectors with respect to the sample around the 180° angle as shown in fig. 4. Alternatively, the detectors can be position-sensitive (Anger cameras) by which a two-dimensional momentum distribution can be measured simultaneously.

The third way of extracting information from positron annihilation is to measure the Doppler broadening of the 511 keV annihilation photons. The photon energy is Doppler-shifted due to the momentum of the electron with which the positron is annihilating. When the electron momentum density inside the sample is somehow distorted, photons with a slightly different energy distribution will be emitted in the annihilation process. This enables to distinguish between different positron states prior to annihilation. The detection system (see fig. 4) is fairly simple and consists of a solid state detector capable of measuring photon energies accurately [3].

The amount of ortho-positronium can be measured from the annihilation γ spectrum in two ways. The more simple parameter is the intensity of the long lifetime of o-Ps. The order way is based on the 3 γ annihilation of o-Ps giving rise to a different energy spectrum of the annihilation radiation than the other annihilation channels that result in 2 γ annihilation.

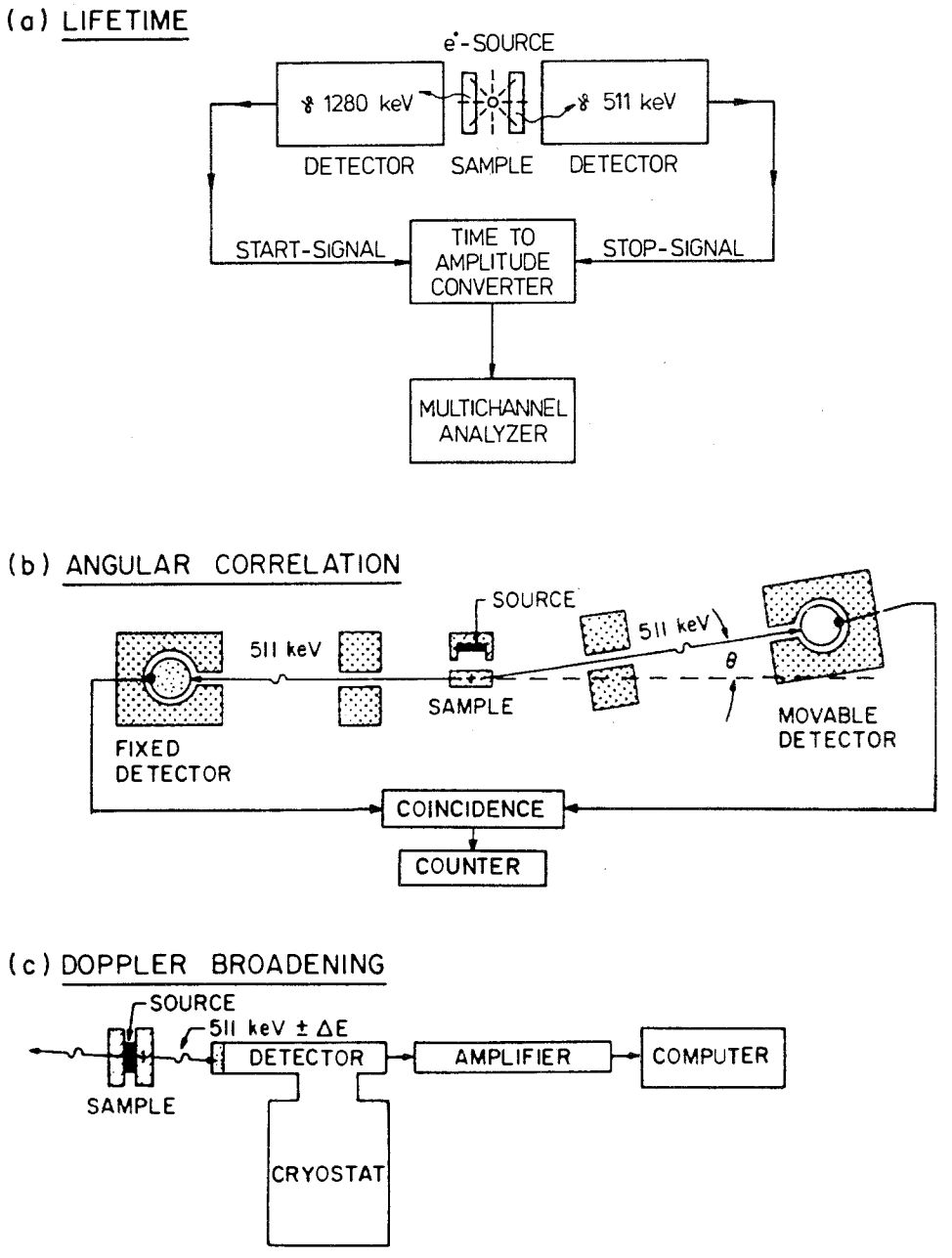

Fig. 4. Schematic diagrams of measuring positron annihilation characteristics. a) The lifetime apparatus consists of two detectors, one of which is tuned to measure the 1280 keV nuclear γ (start) and the other the 511 keV annihilation γ (stop). The time-to-amplitude converter measures the time difference between these two events and stores the value in the memory of a multichannel analyzer. b) The angular correlation of annihilation radiation is measured with one fixed and one movable detector. The coincidences corresponding to the two annihilation γ's from the positron annihilation are measured as a function of the deviation angle θ. c) In the Doppler broadening spectroscopy the energy of the annihilation γ's are measured accurately with a solid state detector.

In positron beam experiments the measured signals can also be positrons after interaction with the solid. Positrons can be detected using channel electron multipliers or, in electrostatic positron beams, using electron energy analyzers.

3.3. POSITRON BEAMS

The key to the generation of a monoenergetic positron beam is the use of a moderator where the high energy positrons from the radioactive source thermalize, diffuse back to the surface and are ejected out with few eV energy due to the negative work function. The source and the moderator are designed to work in the vicinity of each other and form the heart of the beam.

Two different geometrical approaches for the source and the moderator have been used. In the backscattering geometry the moderator is a single crystal and the source is ^{58}Co evaporated onto a high Z substrate. The construction of these small area source-moderator units is fairly simple [24,26]. The other possibility is to use a transmission geometry [27] with a thin foil moderator and an encapsulated ^{22}Na source [28,29]. In one construction the ^{64}Cu isotope has been used, which is evaporated *in situ* on the moderator crystal [30].

Although in the moderation process most of the positrons are lost, the use of a moderator leads to an enormous enhancement of the brightness of the positron beam, as illustrated in the fig. 3. The brightness of the beam can be further increased by re-moderating the positron beam. The best moderators have efficiencies from $3 \cdot 10^{-3}$ [24,26] to $7 \cdot 10^{-3}$ [31]. With a positron source of the

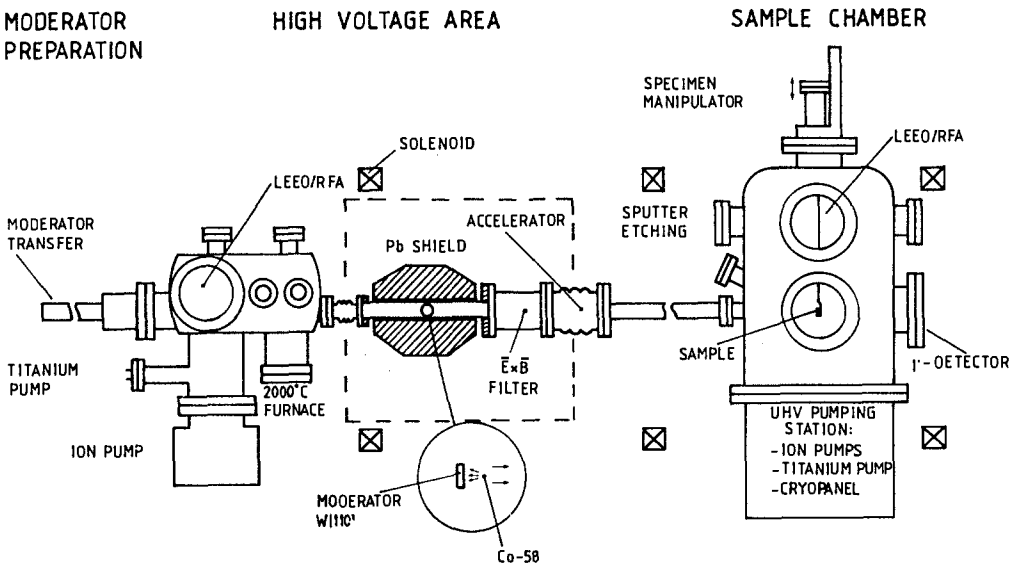

Fig. 5. Schematic drawing of a slow positron beam. Positrons are produced in the radioactive ^{58}Co source, moderated and guided using magnetic and electrostatic fields to the sample chamber. The whole apparatus is designed to work in an UHV environment [26].

order of 100 mCi a positron beam intensity of $1 \ldots 5 \cdot 10^6$ e^+ per second can be obtained.

Transport of the low energy positrons from the moderator to the sample is done using either electric fields or magnetic and electric fields. The construction of a magnetically guided beam is fairly simple and higher beam intensities can be obtained than in the electrostatic beams. The advantage of the more sophisticated electrostatic construction is mainly the absence of magnetic fields that is important when the technique is used in connection with energy dispersive spectroscopies. Fig. 5 shows the schematic drawing of a magnetically guided positron beam in the Helsinki University of Technology.

4. Studying external surfaces with positron beams

4.1. DETERMINATION OF NEAR-SURFACE DEFECT DISTRIBUTIONS

Positron beams are a unique tool for measuring the defect distributions in the near-surface region due to positron trapping at open volume defects. The annihilation radiation can be measured to give information on the internal structure of the defects. Different types of defects can be distinguished, and based on this information the total number of defects can be calculated. The positron annihilation technique with polyenergetic positron sources has been widely used to investigate different types of defects and their evolution during sample treatment [3]. The evolution of monoenergetic positron beams during the last decade has increased the possibilities of positron techniques due to the depth sensitive information obtained by using controlled positron implantation energy [4,7].

Information from the near-surface defect distributions can be obtained by measuring the amount of positrons diffusing back to the entrance surface. The diffusion is reduced by positron trapping into open-volume defects. By measuring the back-diffusion current as a function of the implantation energy the open volume defect distribution can be determined. This method has been applied to studies of vacancy-type defect distributions induced by keV sputtering of virgin Al(110) [32] and Mo(111) [33] surfaces.

Vacancy distributions measured after 0.4 keV and 3 keV Ar^+ sputtering of Mo(111) surface at room temperature are shown in fig. 6. For comparison, calculated vacancy and argon ion distributions are also shown, obtained from Monte-Carlo simulations that can reproduce well the overall shape and spatial extent of the sputtering damage. The interesting observation from these studies is that the defected layer extends several tens of Ångströms from the surface even after sputtering with low energies both in Al and in Mo. Moreover, an amorphous overlayer is observed in the few outermost layers, where the open-volume defect density is of the order of 20 at.-%. The defected layer was observed to recover

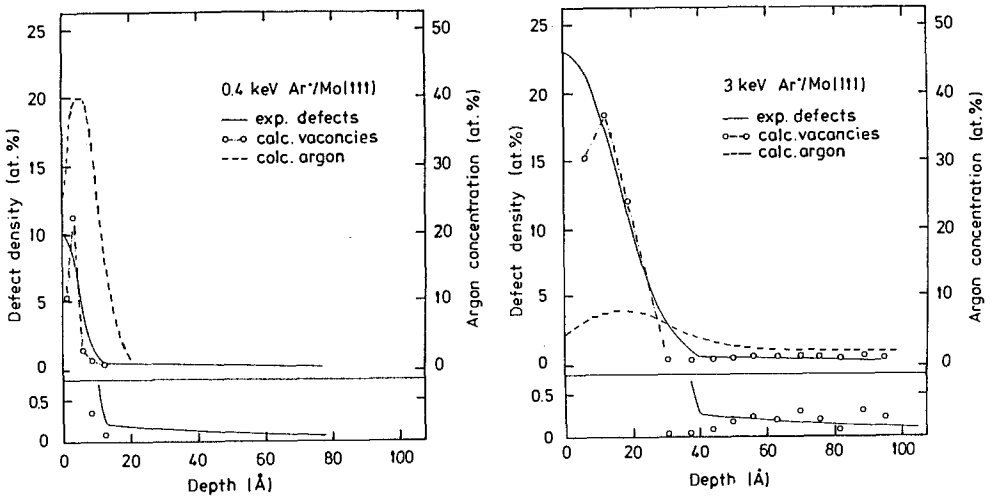

Fig. 6. Extracted vacancy type defect distributions corresponding to 0.4 and 3.0 keV Ar^+ ion bombardment. The width of the damaged overlayer as well as the argon-vacancy ratio is seen to be sensitive to Ar^+ ion energy [33].

after annealing at 750 K in the case of Al(110) and at 900 K in the case of Mo(111).

Re-emitted positron energy spectroscopy (RPS) has been used to study defects in layer structures. The first study in this field [34] was able to identify strong positron trapping sites residing at the interface of the Cu/W(110) system. A strained overlayer was formed during the growth of the first Cu layer on a W(110) substrate containing lattice disorder capable of trapping positrons. These defects were stable far beyond the usual recovery temperatures of point defects in copper. Cobalt film growth on W(110) surface has also been studied with RPS in connection with AES and LEED studies [35]. The Co film growth was commensurate on W(110) up to 1 monolayer and after that a phase transition to Co(0001) was seen with LEED. The positron data indicated that very small number of traps were created at the interface. The authors suggest that the phase transition in the Co/W(110) system leads to an atomically abrupt interface and less open volume to trap positrons.

Huttunen et al. [36,37] have studied the overlayer systems Cu/Ag(111) and Ag/Cu(111). Their results for the open volume defect distribution in the epitaxial layers grown *in situ* are shown in fig. 7. The AES data indicated Stranski-Krastanov growth mode in the Cu/Ag(111) system and layer-by-layer mode in the Ag/Cu(111) system. In the Cu/Ag(111) system they observed approximately three times as many defects. The difference was attributed to the lattice constants ($a_{AG} > a_{Cu}$). When copper is grown on Ag(111) it is more likely that open-volume defects are created than in the opposite system. The defect densities were of the order 10^{18} cm^{-3} which are consistent with electron microscopy results. The defects were confined near the interface. Assuming an exponential reduction as

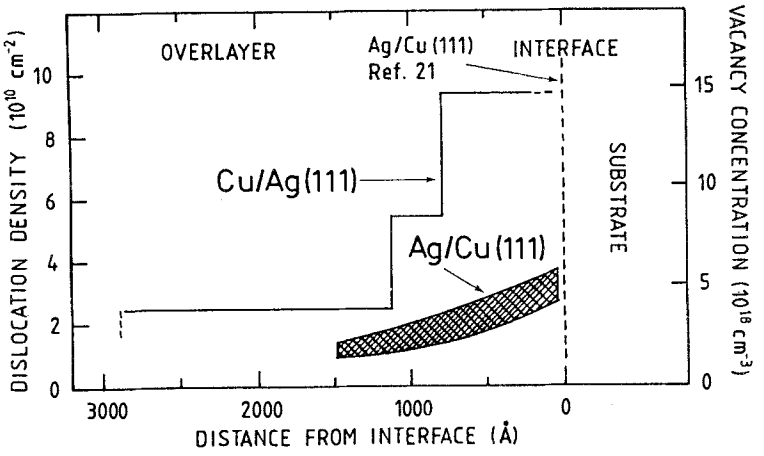

Fig. 7. Extracted defect profiles at Cu/Ag(111) and Ag/Cu(111) interfaces measured with a slow positron beam. The larger amount of defects in the Cu/Ag(111) system can be interpreted in terms of lattice constants ($a_{Ag} > a_{Cu}$) [36].

the overlayer grows, characteristic attenuation lengths of 1500 Å in Cu/Ag(111) system and 1200 Å in Ag/Cu(111) system for the defect densities were found.

When the defected layer is located deeper in the sample a powerful positron parameter is the Doppler-broadened annihilation line shape. The main application of this method has been the studies of ion implantation induced damage in semiconductors. Fig. 8 shows the application of this method to study defects in silicon induced by hydrogen implantation. The data in the figure is obtained from

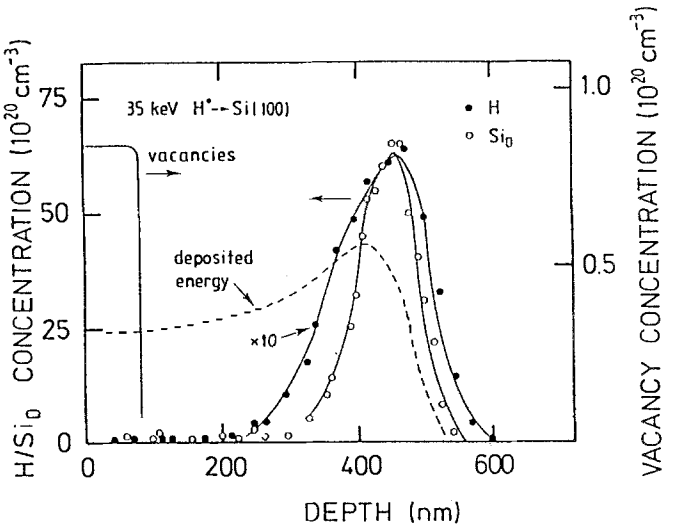

Fig. 8. Hydrogen, displaced Si and vacancy distributions in crystalline Si after 35-keV hydrogen implantation. The dashed line shows the calculated distribution of the deposited energy caused by the nuclear energy loss [38].

a combination of three different methods. The vacancy distribution is extracted from positron beam measurements, the displaced Si atoms from Rutherford backscattering and the amount of interstitial hydrogen from Nuclear Resonance Broadening data [38]. The figure also shows the results of computer simulations for the H and divacancy profiles. A vacancy type damage region is produced in the surface region. In the region of the deposited energy peak, hydrogen is associated with damage consisting of SiH centers and vacancy complexes. In the end region of the damage layer the distribution of the displaced Si atoms is produced by H impurities in the crystal.

The study of hydrogen interaction with oxidized Si(111) surface shows the sensitivity of positrons to interfacial hydrogen at near-surface region. In this study a 20–30 Å thick oxide layer was grown on a Si(111) surface in UHV. This

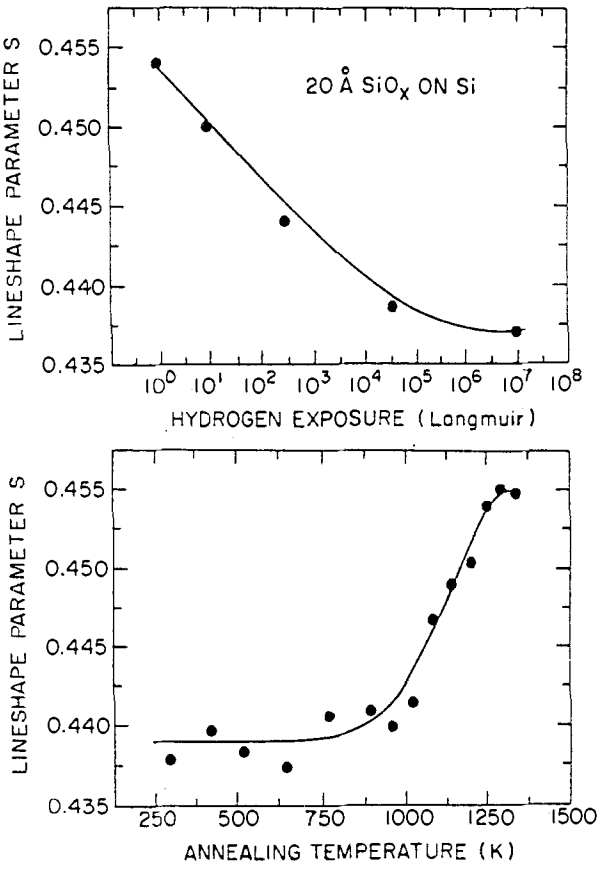

Fig. 9. Positron lineshape parameter S for an oxidized silicon sample. The upper figure shows the change in the S parameter during an initial exposure to hydrogen at room temperature. Changes in S are attributed to the accumulation of hydrogen into the SiO_x/Si(111) interface. The lower part shows the recovery of the hydrogen charged interface during an isochronal annealing after a 10^7 Langmuir H exposure. The initial value of S is retained after a 1300 K anneal. The data is used to extract a hydrogen binding energy of 3 eV to the interface [39].

surface was exposed to hydrogen and after 10 L (1 L = 133 μPa s) a change in the annihilation lineshape (S-parameter) was observed. Saturation of the signal occurs after 10^7 L as can be seen in fig. 9. When this surface was annealed up to 1300 K the measured S-parameter returns to its as-grown value indicating a hydrogen release from the interface. From the hydrogen charging and discharging experiment of the SiO_x/Si overlayer the binding energy of hydrogen in the oxide interface yields $E_B = 3$ eV [39]. This experiment shows the potential of the positron beam technique to measure hydrogen, which with many techniques remains invisible in the near surface region.

4.2. SLOW POSITRONS AS SURFACE PROBES

Electron energy spectroscopies, like low energy electron diffraction (LEED), Auger electron spectroscopy (AES) and electron energy loss spectroscopy (EELS) have established their use as standard tools in surface studies (see e.g. ref. [40]). Positrons can be used instead of electrons in most surface sensitive electron spectroscopies resulting in new analysis techniques. In most cases the experimental setup of the positron counterpart is more complicated but the theoretical calculations become more straightforward due to the lack of exchange interaction. Moreover, the positron beam characteristics, e.g. the brightness of the beam, are comparable with those of electron spectroscopies, sometimes even superior [6]. The positron techniques also provide additional surface sensitive spectroscopies that are unique and are based on the characteristics of the positron or positronium.

Low Energy Positron Diffraction (LEPD) was first demonstrated by Rosenberg et al. in 1980 [8]. In fig. 10 the original data is shown from this experiment, together with theoretical calculations by Read and Lowy [41]. The method has been used to study Cu(111) and Cu(100) surfaces with equipment suitable for both LEPD and LEED measurements [42,43]. The analysis of LEED intensity versus beam energy (I-V) curves indicated first and second layer relaxation. The measured LEPD I-V spectra were in good agreement with the theoretical calculations giving the same structure as the LEED analysis. Similarities and differences between LEED and LEPD results are demonstrated in the isometric plots in fig. 11.

Several authors have compared LEPD and LEED techniques [42,43,45]. LEPD distributions have been found easier to calculate because of the absence of the exchange interaction and the small correlation energy for positrons. In some crystals, like Mo(100) or W(100) where the exchange and correlation terms strongly affect the structural analysis, LEPD is expected to provide valuable complementary information due to the absence of these terms. The elastic mean free path is smaller for positrons than for electrons giving rise to less signal from sub-surface layers. This further affects the required computer time, because the computational time scales roughly as the square of the number of layers. The

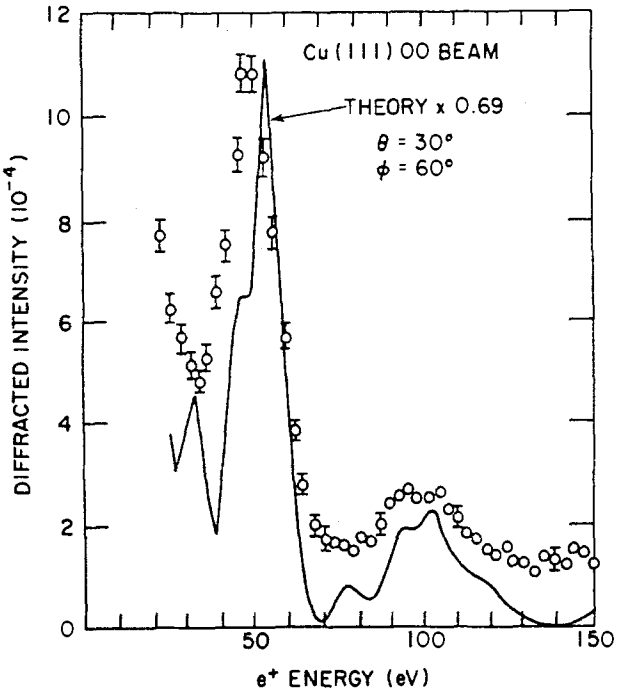

Fig. 10. The diffraction of low energy positron from Cu(111) surface [8]. The solid line represents a theoretical calculation by Read and Lowy [41].

cross section for elastic scattering is also weaker for positrons than for electrons, giving rise to reduced multiple scattering. However, the LEPD calculations require the use of dynamical theory [43], although a simple kinematic picture has been found valid in NaF and LiF [45]. The disadvantages of LEPD are the more complicated apparatus and the lack of established reference data. To obtain more complete information from the surface structure both methods should be used simultaneously.

Positrons trapped by the potential minimum at the surface (see fig. 1) can annihilate with the core-electrons creating a core-hole excitation which can then relax via the familiar Auger-process. This position annihilation induced Auger-electron spectroscopy (PAES) was recently demonstrated by Weiss et al. [9]. In fig. 12 the PAES spectrum from a polycrystalline Cu surface is shown. The energy of the incoming beam is 20 eV and the outcoming electrons can be attributed to the $M_{23}M_{45}M_{45}$ Auger transition.

The advantages of this novel technique when compared to conventional AES are that low-energy positrons (below 50 eV) are used to remove core-electrons by matter-antimatter annihilation instead of a keV energy electron beam. Electrons cause damage to organic systems, charging problems in insulators and desorption of adsorbed layers, which are well known limitations of the conventional Auger-spectroscopy. The scattered primary and secondary electrons also give rise to a

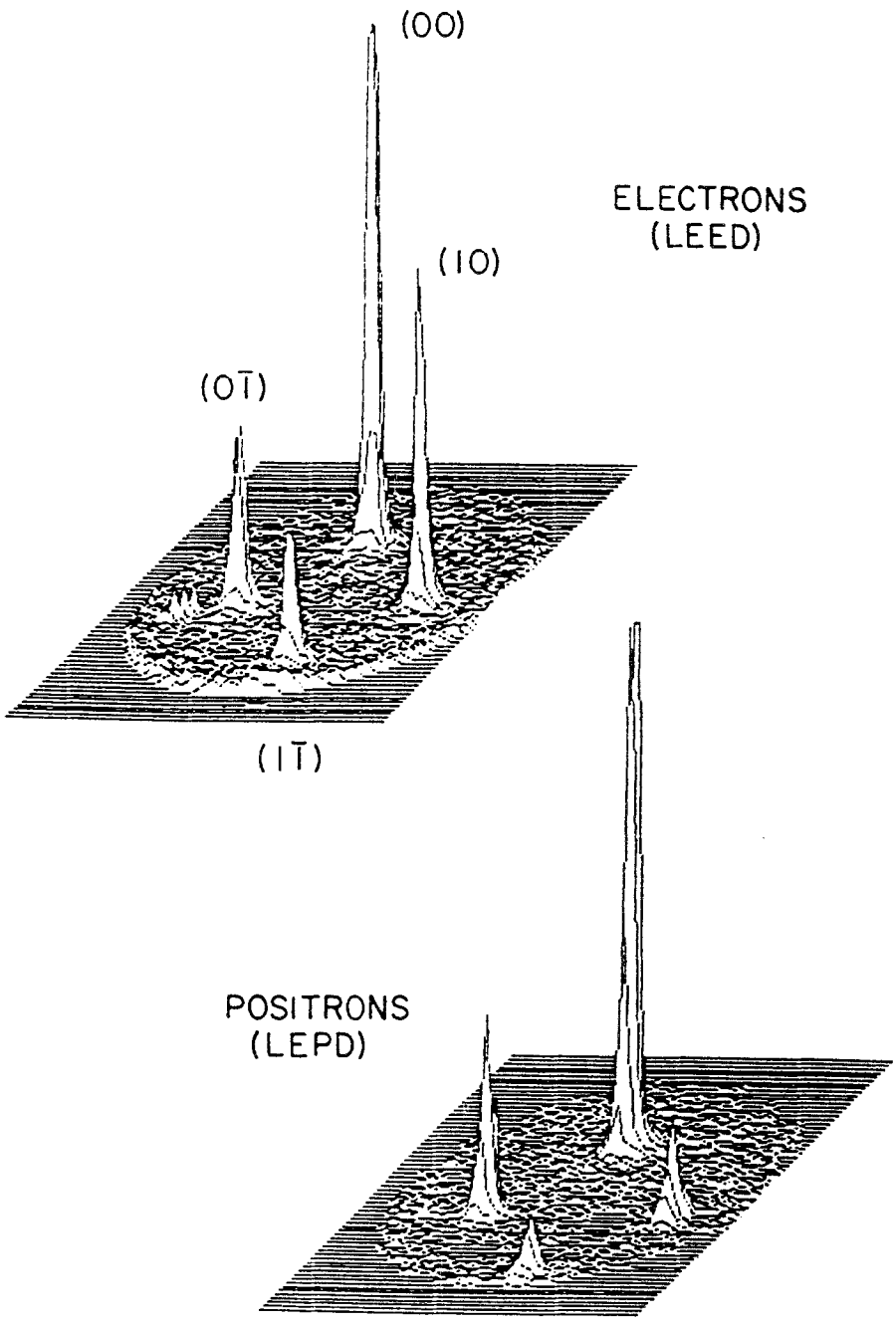

Fig. 11. Isometric plots comparing low-energy diffraction results for electrons and positrons [44].

non-linear background in the Auger-spectra. When the positron beam is used to induce the Auger-process, the positron energy is low enough not to damage the surface or create any secondary electron background. The energetic electron

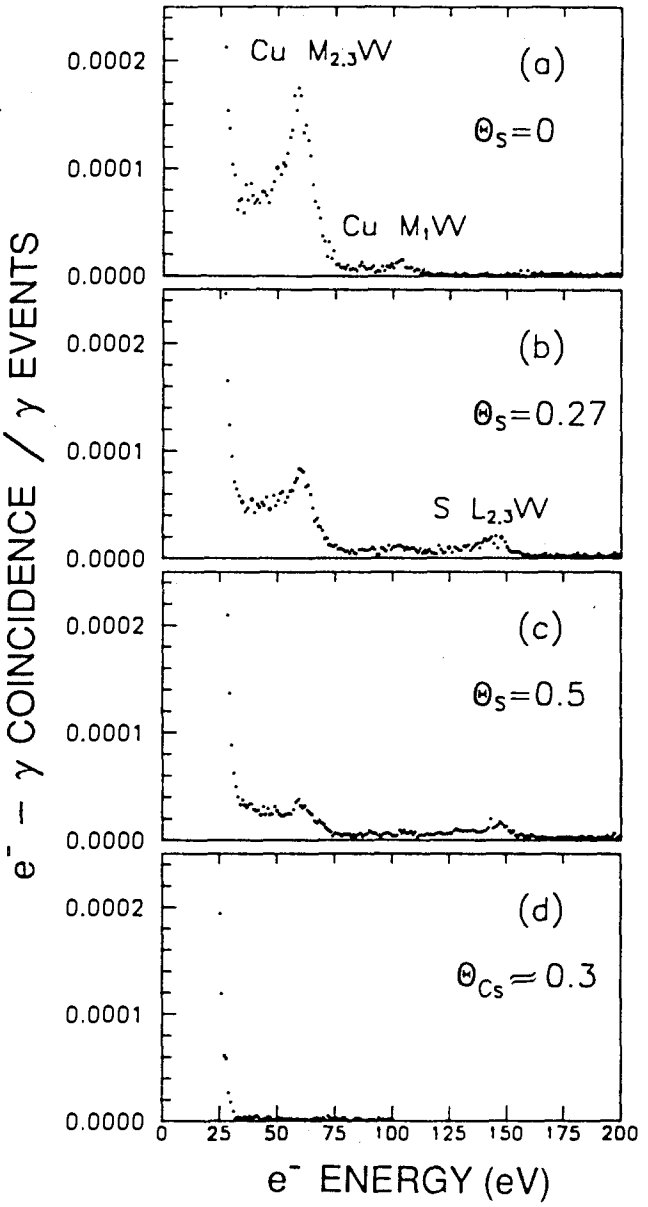

Fig. 12. Positron annihilation induced Auger spectra from Cu surfaces. (a) represents the spectra of a clean surface, in (b) and (c) 0.27 and 0.5 monolayer *S* is deposited, respectively and in (d) a saturation coverage of Cs has been evaporated on the surface [46].

beam also excites the atoms deep below the surface. Although the short escape depth of Auger-electrons provides surface sensitivity, the signal normally becomes an average over several atomic layers. Because the positron is trapped at the surface before annihilation with the core-electron, the Auger-electrons emitted come from the outmost layer providing extreme surface sensitivity.

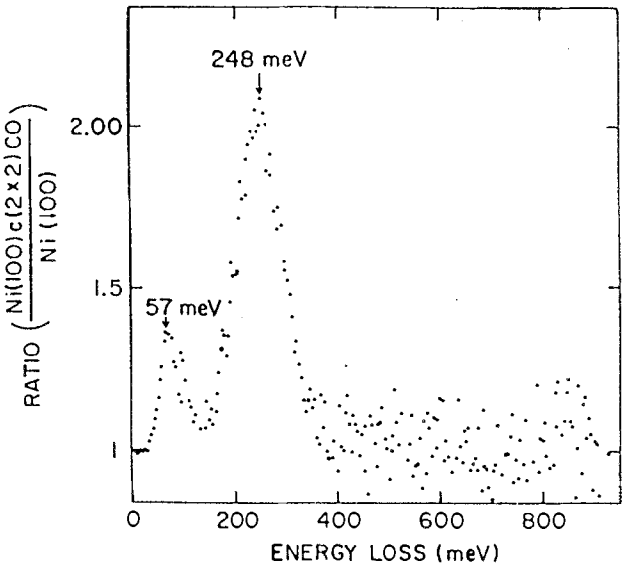

Fig. 13. Re-emitted positron energy loss spectrum from CO on Ni(100). The data is the ratio of Ni(100)$c(2\times2)$CO to clean Ni(100), showing energy loss peaks for Ni–C (57 meV) and C–O stretch (248 meV) [48].

The PAES apparatus has been described in detail recently [47] and it has been applied to study sulphur and cesium deposition on Cu as demonstrated in fig. 12. This study shows clearly the surface sensitivity of this technique. As can be seen from the figure, 0.5 monolayer of S on Cu(110) surface was enough to reduce the Cu signal. The intensity of the Cu $M_{2,3}W$ line goes linearly to zero when the S coverage approaches one monolayer. Alkali metals suppress the substrate signal even more: 0.3 monolayer of Cs on Cu(110) causes a total disappearance of the Cu signal. The surface sensitivity is due to the feature that positrons can be used selectively to excite Auger transitions from the topmost atomic layer [46].

An interesting application of measuring the energy distribution of the re-emitted positrons is utilized in the technique named REPELS (re-emitted positron energy loss spectroscopy). This technique, which is analogous to EELS, was first demonstrated by Fischer et al. [48]. The measured REPELS spectrum from CO on Ni(100) is shown in fig. 13. The authors have also measured S, C and O deposited on various metals and H_2O on NiO(111) [49]. The measured energy-loss peak at 248 meV for CO on Ni(100) agrees with EELS data for C-O stretching. The loss peaks after 2 L of H_2O on NiO(111) at 23 K were found at 110 meV (H_2O rotation), 220 meV (H bonding) and 400 meV (O-H stretch). The advantages of this technique are the good sensitivity to very small energy losses and the absence of exchange effects, which may be important when adsorption of paramagnetic molecules is studied.

Transmission electron microscopy (TEM) is a widely used imaging technique for thin film applications. The transmission positron microscope (TPM) has been

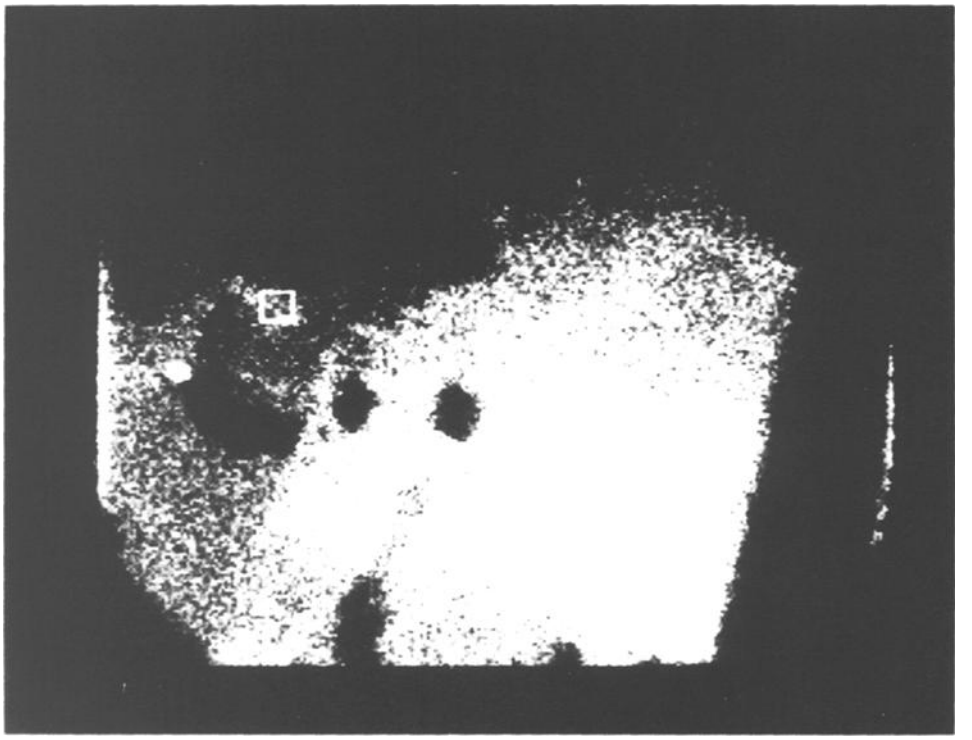

Fig. 14. A 115× magnification PRM image of a Ni(100) film. The white parts represent positron re-emission and thus defect free regions. Three segments of the hexagonal support mesh are visible at the right and lower parts of the figure [50].

introduced [11] and works in a similar manner to TEM. The only difference in TPM is the use of positrons instead of electrons. A subsequent step was the positron re-emission microscope (PRM) that has no electron counterpart [12]. The PRM utilizes positrons implanted within the diffusion length from the sample surface, that are thermalized in the bulk and ejected out from the surface because of the negative work function. The re-emitted positrons are accelerated and focused to form an image of the surface. The PRM is sensitive to surface and near surface defects. This device has been used to study sputtering induced defects on Mo and W surfaces. The re-emission from the damaged parts of the surface was found to decrease drastically due to the trapping of positrons in the defects. The positron microprobe [50] is an advanced PRM with double re-moderation to increase the brightness of the positrons. In fig. 14 a PRM image is shown from an epitaxially grown 150 nm thick Ni film on Ni(100) surface. This image was taken with ×115 magnification. The bright parts represent positron re-emission and thus defect free regions. The dark spots represent regions where positrons are trapped at or near the surface. The picture is bordered at the right and lower right by the shadows of three segments of the hexagonal support mesh.

The resolution of the technique is limited by the deBroglie wavelength of positrons which is about 20 nm at room temperature. The PRM device has a potential of working with a beam size of the order of 1 nm, and if positrons that are emitted before thermalization are used the smaller beam size can be utilized in a totally new era of research [22].

The applications of PRM in the studies of model catalyst surfaces has been proposed [51]. The sample thickness for TEM analysis has to be less than 10 nm which makes the samples very fragile, but for PRM the substrate thickness plays no role in the analysis. The PRM contrast mechanisms can depend much more strongly on the adsorbate Z, on islanding of the overlayer and alloying of the metals involved and also on the defect concentration on the surface. Such information on model catalysts are of extreme importance when real catalysts are constructed. Recently, positron tunneling microscopy (PTM) as the counterpart for scanning tunneling microscopy (STM) has been proposed [52]. The method is based on positrons tunneling through the thin overlayer film on solid surface. Information on the growth and imperfections of the overlayer can be obtained.

The effect of surface steps on Ni(110) has been studied by Köymen et al. [53]. They produced variable amount of steps by evaporating Ni on the Ni(110) substrate and by Ar^+ sputtering followed by annealing at various temperatures. Fig. 15 shows the positronium formation fraction as a function of surface ledge size derived from the sputtering-annealing experiments. The step density was determined by measuring the broadening of the LEED spot profiles. Positronium formation on the surface was observed to be sensitive beyond the detection limit (coherence length) of the LEED gun and new information was obtained on the island nucleation density of Ni on Ni(110) system. The combination of LEED with positronium formation on the surface can be a useful tool in determining the surface defects because LEED is useful when the defect spacing is below 200 Å, whereas the positronium technique is most sensitive when the defect spacing exceeds 200 Å.

Angular correlation of annihilation radiation (ACAR) connected with positron beams has been applied to study the electronic structure of copper [54], aluminum [55], silicon [56], graphite [57] and lead [58] surfaces. This technique is an ideal instrument for measuring the electron momentum parallel to the surface. From the ACAR spectra the parallel and perpendicular momentum component of positronium formed with surface electrons and annihilating at the surface can be separated. The electron momentum can then be calculated from the measured momentum distribution of positronium. The reconstructed Si(111) 7×7 surface has also been studied using 2D ACAR [56]. The results indicate that positrons are annihilating at the surface with electrons whose momentum are similar to that of bulk electrons. The potential of 2D ACAR technique in studies of the nature of surface electronic structure still remains to be developed in the future.

The temperature dependence of e^+ and Ps emission have been studied for several surfaces [10,59,60,61], and the result from Cu(111) surface is shown in fig.

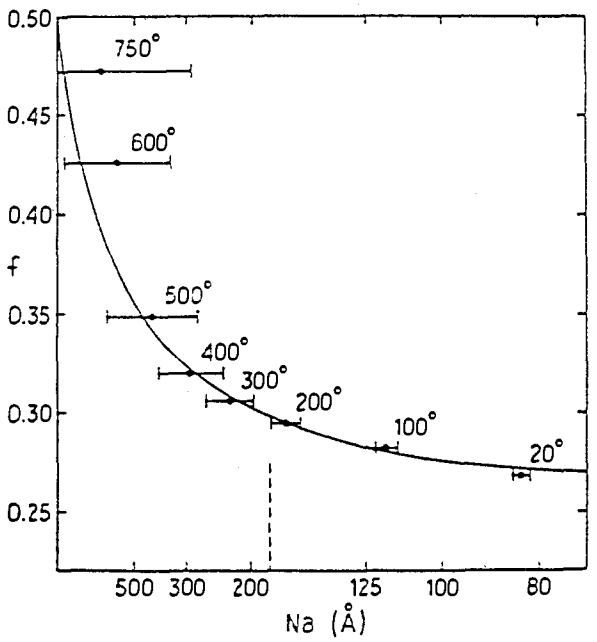

Fig. 15. The positronium fraction as a function of the surface terrace width, Na, determined by LEED for Ni(110). The surface was prepared by Ar^+ sputtering followed by annealing at different temperatures given in the figure in °C. The coherence limit of the LEED system is shown with a dashed line [53].

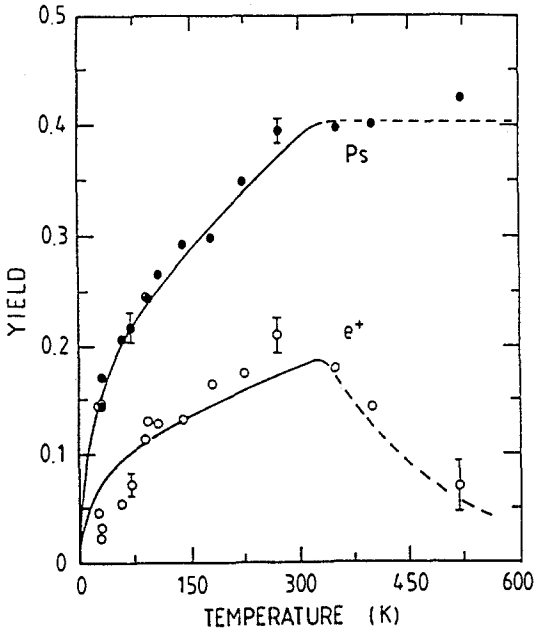

Fig. 16. Positron and positronium emission after zero incident energy implantation as a function of temperature at Cu(111) surface. All emission channels at the surface are closed at 0 K. The data suggests more generally that the sticking probability of low energy particles approaching the surface vanishes at 0 K [59].

16. The results were explained in terms of a simple transmission model where the surface potential was a standard one-dimensional image-induced potential, and the positron was described with a plane-wave, weighted by a thermal energy distribution. The interpretation of the data suggests that positron penetration trough the surface potential is responsible for all the temperature dependence, and the Ps formation can be regarded as a separate temperature independent process. The results also suggest more generally that the sticking probability of low-energy particles approaching the surface vanishes at 0 K [59].

Surface magnetism has been studied by Gidley et al. [62] by using a polarized positron beam. The positronium formation can take place only outside the material, about 2 Å away from the ion cores, providing extreme surface sensitivity. The authors were able to measure the critical exponent for the temperature dependence of polarization of electrons at the Ni(110) surface. The measured value of 0.7 is consistent with model calculations and other experimental data. They also observed that adsorption of 0.5 monolayer O_2 on the surface is sufficient to quench the ferromagnetic order at the surface.

4.3. STUDYING ADSORBATE SYSTEMS WITH SLOW POSITRONS

Thin overlayers and adsorbate systems have been studied by measuring positron back-diffusion, positronium formation, angular correlation of annihilation radiation and positron lifetime at the surface. In principle all the methods described in previous sections can also be used to study adsorbate systems. The techniques have unique potential that has been utilized very modestly.

Submonolayer coverage of alkali metals have been seen to enhance positronium desorption from Ni(100) and Ni(110) surface [63]. The activation energy for desorption decreases almost linearly with increasing alkali coverage in the case of Na on Ni(100) and Cs on Ni(110). The amount of positronium formed at the surface is reported to increase with the alkali coverage. The increase can be explained by lowering of the electron work function and increase of the electron density at the surface due to alkali atoms.

It has been observed that positrons are suitable to study structural imperfections on the surface. The first demonstration of this type of study was made by Lynn [64] from Al_xO_y growth during oxygenation of Al(111) surface.

The oxygenation of Al surfaces has also been studied with ACAR [55]. The method showed a remarkable sensitivity to oxygen contamination even below 0.1% of a monolayer on Al(100) surfaces. Exposing the surface to 150 L of oxygen, which corresponds to one monolayer of O on Al(100), an increase in the Ps formation by 5% was seen together with narrowing of the Ps momentum distribution. At 3000 L an overlayer oxide was grown on the Al(111) surface and the Ps spectrum mainly reflected the electronic properties of the oxide. When the exposure was increased to $1 \cdot 10^6$ L the Ps emission dropped almost to zero indicating that positrons were trapped in the disordered oxide layers or possibly

in the interface region due to increased thickness of the Al-oxide layer (10 Å). The results imply that the positronium 2D ACAR spectrum might offer a new angle-resolved surface-sensitive spectroscopy. Since the final state of the Ps formation is well defined (e^+–e^- bound state), this technique has an advantage over the angle-resolved photoemission where free electron final states are normally assumed in order to map out the band dispersion of initial states [6].

The evolution from the chemisorption of oxygen on Si(111) surface to the formation of a SiO_2-like compound has been observed by measuring both the e^+ reflectivity and Ps formation probability versus positron incident energy [65]. Spectral features can be associated with changes of the near-surface electronic structure. The band gap affects both the positron thermalization and the positronium formation and can be utilized to detect nondestructively changes in surface electron density of states in the near-surface region.

Like the electron work-function the positron work-function can give information on the changes at the surface due to different kind of treatments. The integral energy distribution for positrons re-emitted from various surfaces have been measured with and without adsorbates and the data is collected in ref. [6]. There is still, however, insufficient data from well-characterized surfaces to fully understand why the positron re-emission process is inelastic in some cases.

5. Studying internal surfaces with polyenergetic positrons

It is relatively difficult to obtain direct information on the internal surfaces of porous catalysts. Methods that are normally used in surface characterization of low-area catalysts can detect only a very small fraction of the active area of industrial catalysts. The internal surfaces can be detected only by methods where photons that are not interacting with the medium carry the information to the detection system. Methods like infrared or Mössbauer spectroscopy have been applied to this field [66].

Positronium annihilation spectroscopy (PAS) [5,14] is an in-situ surface sensitive method, by which the properties of the internal volume of porous catalysts can be probed. The schematic setup for the technique is given in fig. 17. In PAS high-energy positrons from a radioactive isotope are directly implanted into the studied system. Due to the continuous energy spectrum of positrons a broad implantation depth distribution is obtained. Positrons thermalized inside the insulating material have a relatively high probability to form positronium while diffusing into the vacuum. The kinetic energy of emitted Ps atom is given by eq. (2). In vacuum the Ps atom is bouncing inside the cavities until it hits a chemically active site giving rise to pick-off annihilation.

The Ps formed inside the sample can be detected by measuring the relative intensity and lifetime of the long lifetime component of the annihilation radiation. The o-Ps atom lifetime in vacuum is 142 ns. The lifetime can be shortened

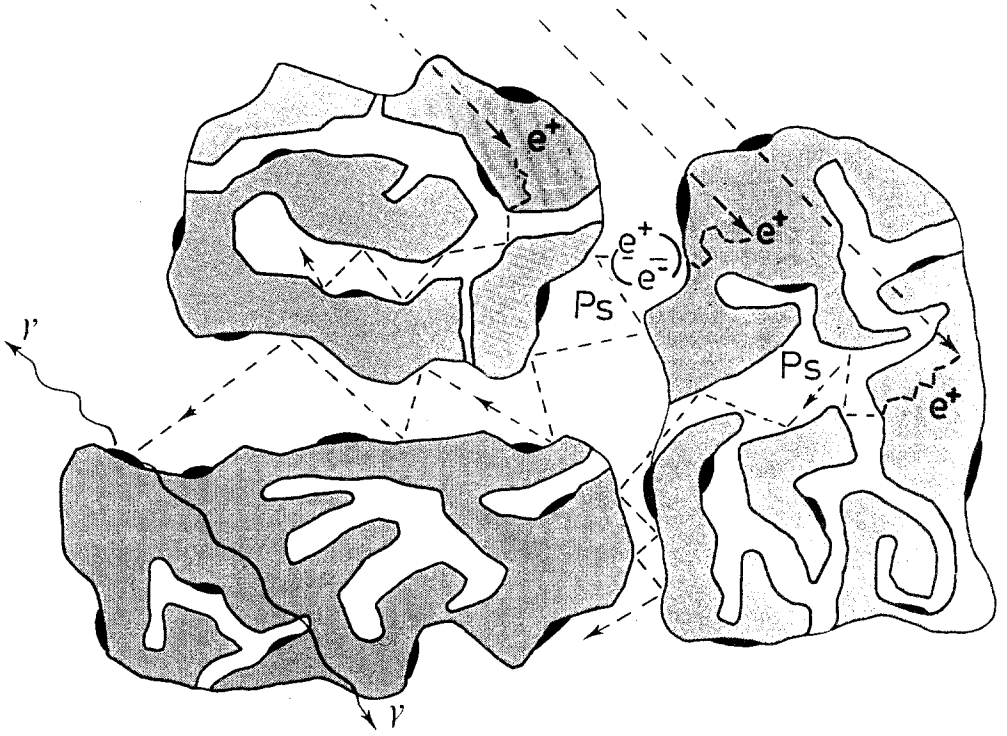

Fig. 17. The schematic setup for positronium annihilation experiment for catalyst characterization. Positrons obtained from radioactive source slow down inside the material and some of them form Ps-atoms at the surface. The Ps-atoms can not penetrate back into the grains but are reflected from the surface. The lifetime and traveling distance of Ps is restricted either by the collisions with metal atoms able to give an electron or by the self annihilation after 142 ns in vacuum. The information on the internal surfaces is carried to the detection system by the 511 keV γ radiation.

by the pick-off annihilation, where the Ps atom interacts with a free electron causing the annihilation. In an environment where the amount of free electrons is very small, like inside the internal voids of metal oxide powder, the lifetime is nearly as long as in vacuum. During its lifetime the o-Ps atom travels a distance of the order of 10 cm in the internal pores and it can not penetrate inside the metal oxide grains. The information is obtained as a volume average within the sample, in contrast from only the few topmost atomic layers in the case of electron spectroscopies.

One additional problem faced with insulators is that they become electrically charged when electron spectroscopies are used. In PAS the dose of electric charge is very small and, moreover, the Ps atom, as a neutral particle is not influenced by any amount of charge.

To utilize the PAS method the surface area of the catalyst, the chemical reactivities of adsorbed species and the concentration and chemical state of impregnated metals can be correlated with the o-Ps lifetime characteristics [14].

The ortho-positronium lifetime is normally measured as a function of some impurities causing the pick-off annihilation in the carrier material. The annihilation rate λ is the inverse of the lifetime and it depends on the concentration c according to

$$\lambda = \lambda_0 + kc. \tag{3}$$

The λ_0 is the annihilation rate without any additives and k is the proportionality factor.

A more detailed review about positron and positronium chemistry has recently been published [14]. In this review positron and positronium annihilation in liquids and gases as well as in molecular solids are discussed. Also the applications to biological systems and in the study of phase transitions and other structural studies in micellar systems, microemulsions and polymers are described.

5.1. STUDIES OF CATALYST CARRIER MATERIALS

Positronium lifetime measurements can be used to measure the surface area or pore radius of the high area carrier materials. The surface area of porous resins has been studied using Ps annihilation by Venkateswaran et al. [67]. In fig. 18 is

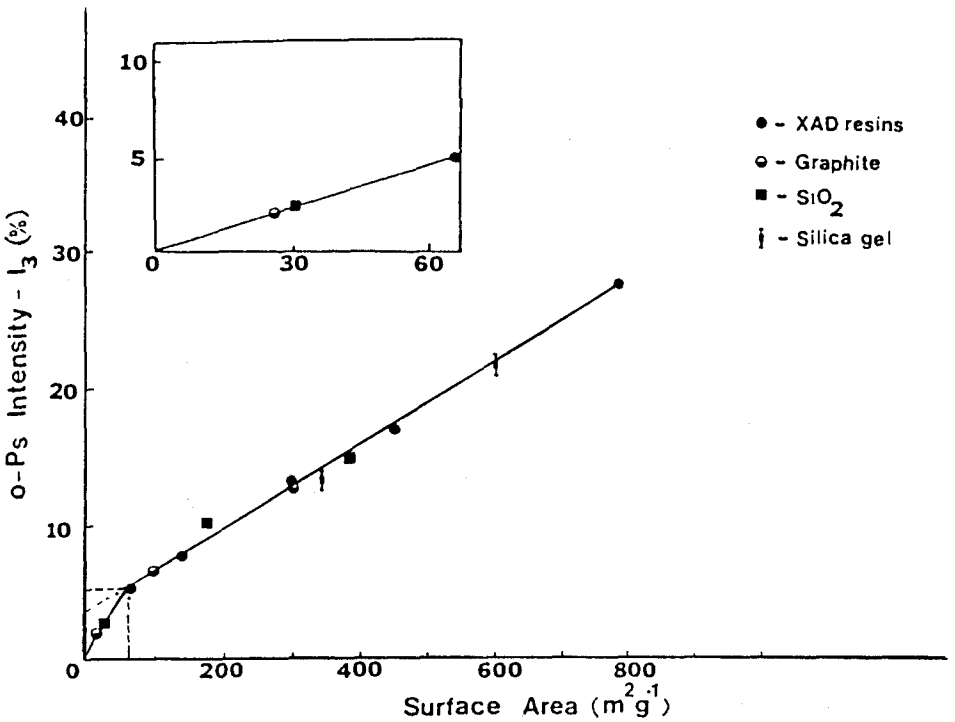

Fig. 18. The o-Ps intensity as a function of surface area. The amount of o-Ps formed at the surface of the sample is clearly a linear function of the internal surface area [67].

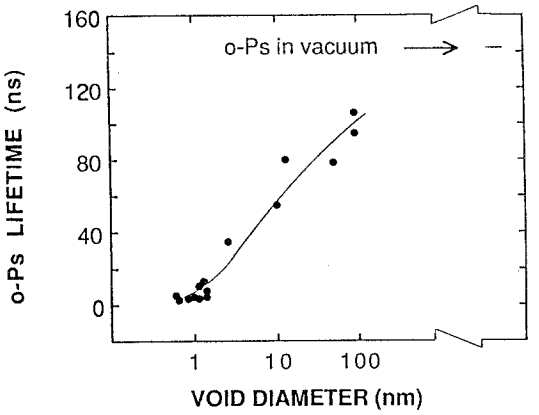

Fig. 19. The lifetime of o-Ps as a function of internal pore diameter. The o-Ps lifetime data has been collected from refs. [67] and [69] and references therein.

shown their collection of the ortho-positronium intensity data as a function of surface area for different zeolites. The o-Ps intensity in the XAD resins as well as other high surface area materials was reported to correlate well with the BET (Brunauer-Emmet-Teller)-surface area. The measurement of surface area with o-Ps formation is based on the formation of Ps from thermalized positrons at the surface.

The o-Ps lifetime was reported to correlate with the pore radius in low polarity XAD-2, XAD-4 and XAD-7 resins. For XAD-11 and XAD-12, where amide and nitroso groups exist on the surface, the quenching of o-Ps increases and the correlation between o-Ps lifetime and the pore radius breaks off [67]. Ito et al. have measured the o-Ps lifetimes in A-type, 13X and ZSM-5 zeolites and found a similar correlation between the lifetime and the diameter of the internal voids [68,69]. In the latter case the void size of the samples was below 1 nm, close to the ultimate resolution of transmission electron microscope. A summary of the data is drawn in fig. 19. By performing magnetic quenching experiments they were also able to separate two different o-Ps lifetime components. The shorter originates from the regular voids of the material and the longer was attributed to the o-Ps annihilating in the inter-particle open space [69].

Nakanishi and Ujihira [70] have studied zeolites using positronium lifetime and Doppler broadening spectroscopies. They have studied the 13X synthetic zeolite that exhibits a lifetime of 8 ns with a pore radius of 6.6 Å. A longer lifetime of 50 ns was also found in the measurements and was addressed to 60 Å pores which exist irregularly in the faujasite zeolites. The o-Ps lifetime in the cages was found to become longer as the desorption of water molecules proceeded indicating that adsorbed water molecules or OH groups can quench o-Ps. Ion exchange of the zeolites was done to study the effect of Brønsted acidity on the o-Ps lifetime. Based on the smaller o-Ps lifetime it was suggested that the NH_4 substituted zeolites have smaller cage volume than the original zeolites. Brønsted acid sites

were found to have a double effect on the o-Ps lifetime: they can act as an oxidizer of o-Ps and also inhibit the Ps formation. According to the authors the estimates of acidity obtained from positron measurements seem to agree with the results obtained from IR spectroscopy.

Debowska et al. have investigated the de-alumination of Y zeolites [71]. The o-Ps lifetime has been reported to increase as the de-alumination proceeds. The interpretation of the phenomena is not clear but it can be assigned to changes in the crystalline structure or in the electronic environment at the surface. A similar effect has also been seen in A- and faujasite-type zeolites with different SiO_2/Al_2O_3 ratios [72].

We have done o-Ps lifetime measurements in different kinds of alumina support materials [73]. The overall shape of the lifetime spectra from supports that have a 200 m^2/g surface area indicate a sum of several different lifetimes. Obviously several pore sizes exist in a high surface area material. On the other hand, the 100 m^2/g surface area support, having a more homogeneous pore size distribution, exhibited a more one-component-like lifetime behavior. As mentioned earlier, the o-Ps atom has a high reflection coefficient at alumina surfaces. The reflectivity was estimated using Monte-Carlo calculations to be 0.99999, indicating that o-Ps atom does not react with the inert metal oxide surface.

As a summary, the o-Ps lifetime has been found to correlate with the inner void size of oxide materials. Changes in the o-Ps lifetime due to different treatments have been attributed to the changes in the pore size. A full exploitation of the method to studies of pore size distributions is still under development.

5.2. THE EFFECT OF METAL IMPREGNATION

The effect of metals impregnated on different carrier materials has been studied with o-Ps lifetime spectroscopy. The method is based on the different electron structure of the carrier material and the deposited metal atoms. Positrons are reflected very effectively from the carrier material, whereas the collision with a metal atom ends up in annihilation. The effect of metal concentration can be calculated by using eq. (3).

Lou et al. [74] have measured the chemical reaction rate constants between positronium atoms and γ-alumina supported metal catalysts. The reactivity correlates with the reduction potential for single electron transfer reactions. For K and Na the reactivity seems to be zero and for Co, Cr, Ni and Fe the reaction rate increases in this order. Also silica and alumina supported palladium has been studied [75].

We have done o-Ps lifetime measurements in alumina supported Pt, Co and Ni catalysts and measured the dependence of the annihilation rate on the metal concentration after impregnation [73]. The measured concentration dependence of the o-Ps annihilation rate in Pt/Al_2O_3 and Co/Al_2O_3 systems is shown in fig. 20. The method is sensitive for Pt concentration below 200 ppm, whereas for Co

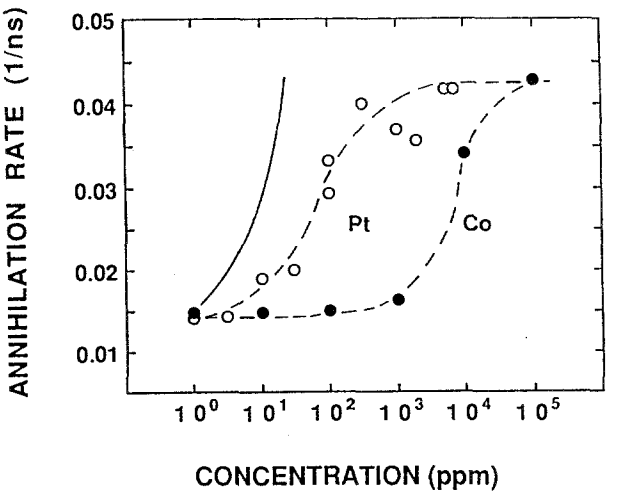

Fig. 20. The ortho-positronium annihilation rate as a function of metal concentration on the internal surfaces of an alumina carrier. The sensitive concentrations are for Pt below 200 ppm and for Co from 0.1 to 10%. The dashed lines through the data points are drawn to guide the eye. The solid line shows the result of a Monte-Carlo simulation where single metal atoms are deposited on the internal surfaces [73].

and Ni the sensitive range is from 0.1% to 10%. The extreme sensitivity for Pt is due to the high dispersion and easy reduction of noble metals inside the cavities. In the case of less noble Co or Ni the metal atoms are oxidized, and as such they have a high reflection probability for o-Ps collisions, similar to the support material. Only a small amount of Co or Ni atoms are in a metallic state and give rise to pick-off annihilation. The results were also simulated with Monte-Carlo calculations, where single active sites, able to quench the Ps atoms, were deposited on the internal surface of the cavities. The results of these calculations are shown in fig. 20 with the solid line, indicating that the noble Pt atoms are dispersed on the internal surfaces almost ideally.

Mogensen et al. [76] have studied silica supported iron catalysts using lifetime and Doppler-broadening experiments. In pure silica they observed a long o-Ps lifetime that disappeared after Fe impregnation due to pick-off annihilation. Oxidation of the surface leads to reappearance of the long o-Ps lifetime components supporting our interpretation that transition metal oxides can be distinguished from metallic states inside a supported catalyst.

5.3. STUDIES OF ADSORPTION

The effect of adsorption of simple gases on the surface of zeolites have also been studied using o-Ps lifetime and Doppler-broadening of the annihilation line. The possibility to study chemisorption has been proposed by Mokrushin [77]. The annihilation rate of o-Ps increases with the increasing equilibrium gas pressure as

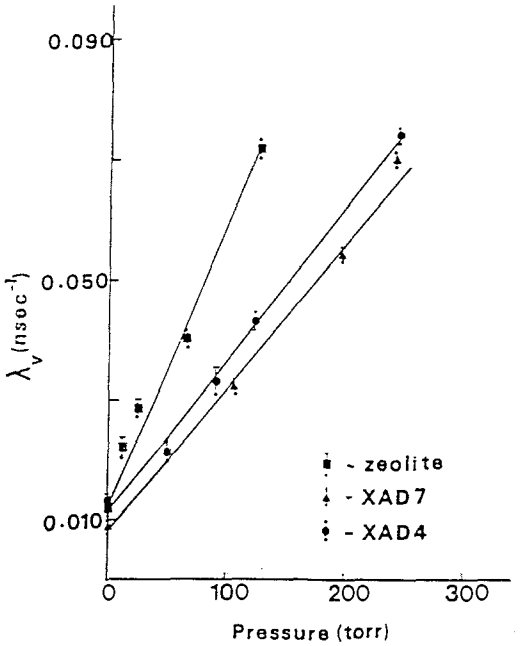

Fig. 21. The ortho-positronium annihilation rate as a function of the equilibrium pressure of NO_2 molecules in a porous material. The annihilation rate is defined as the inverse of the lifetime [78].

predicted by eq. (3). The adsorbed gas on the surface of high area materials has a double effect: it can inhibit the o-Ps formation and quench the o-Ps lifetimes, both of which cause a decrease in the o-Ps signals.

Fig. 21 shows the o-Ps annihilation rate as a function of NO_2 pressure [78]. From the lifetime data two separate reaction rate values can be calculated. The reaction rate of o-Ps with adsorbed gas on the surface is found to be higher than the reactivity with the gas inside the cavities. The observed chemical reactivity of positronium with gas molecules inside the voids is found to be a few orders of magnitude less than those reported in a free gas. The reaction of Ps with adsorbed NO_2 or SO_2 on zeolites should be written as [78]

$$\mathrm{Ps} + \mathrm{XO_2^-} \leftrightarrow \mathrm{PsXO_2^-} \rightarrow 2\gamma, \tag{5}$$

and it also holds for oxygen [68]. In the case of NO the reaction mechanism is not fully understood [79].

Arefev et al. [80] have studied the NaA zeolite by measuring the annihilation lifetime of positrons and the angular distribution of annihilation photons. They were able to measure the void size in water, ice and Se filled NaA zeolite. In the case of water or ice the void size is reduced from 11 Å to less than 3 Å and in the case of Se a value of 5 Å is obtained, which is only a little larger than the value 3.5 Å corresponding to the intermolecular distance of a-Se.

Adsorption of nitrogen [81,82] and methane [83,84] on graphite has been studied using lifetime and Doppler-broadening experiments. The annihilation

lifetime increases with the N_2 coverage at 77 K up to half of a monolayer and after that decreases below the initial value. In the case of CH_4 the changes occur between coverages from 1 to 1.5 of a monolayer at 77 K. The lifetime was also found to be sensitive to the adsorption temperature. From these studies it can be concluded that positronium is sensitive to adsorbed gases on the surface and a dependence of annihilation characteristics on coverage can be seen.

6. Conclusions

Applications of the positron technique to study solid surface have been described in this review. The positron as a positively charged particle is sensitive to the changes in the electronic and atomic density. The γ radiation obtained from positrons annihilating with electrons carries information on the state of both particles before annihilation. By measuring the positron lifetime, the Doppler broadening or the angular correlation of the annihilation radiation information on the electron environment inside the sample can be obtained.

Monoenergetic positrons give information on the surface and near-surface region. The technique is sensitive to open-volume defects, such as vacancies inside the sample or at the surface. With positron beams new techniques as counterparts for electron induced surface sensitive techniques have been developed. Positron annihilation induced Auger-electron spectroscopy has been found to be very sensitive to the adsorbed species at the outermost atomic layer. Low energy positron diffraction can be used together with LEED to obtain complementary information on the surface structure. Positron re-emission microscopy is sensitive to the near-surface defects.

Positronium annihilation has been used to study the internal surfaces of porous catalysts. It has been found that the technique is sensitive to the size of the internal volume and the surface area of the porous material. With o-Ps lifetime measurements metal impregnation and adsorption of gases can be studied.

In summary, positron techniques include a wide variety of different techniques by which plenty of information can be obtained on surfaces but their applications to catalytic studies have been quite modest. The techniques have been applied to surface and near-surface studies of crystalline samples and to surface studies of internal surfaces of porous materials.

Acknowledgments

We are indebted to K. Canter and Y.C. Jean and D.W. Gidley for submission of their manuscripts and other relevant information. We would also like to thank J. Mäkinen and K. Rytsölä for their comments on the manuscript.

References

[1] C.D. Anderson, Phys Rev. 43 (1933) 491.
[2] Y.C. Jean, R.M. Lambrecht and D. Horváth, *Positrons and Positronium, a bibliography 1930–1984*, Physical Science Data, Vol. 33 (Elsevier, Amsterdam, 1988).
[3] *Positrons in Solids*, ed. P. Hautojärvi, Topics in Current Physics, Vol. 12 (Springer-Verlag, 1979).
[4] *Positron Solid State Physics*, eds. W. Brandt and A. Dupasquier (North-Holland, Amsterdam, 1983).
[5] K.L. Cheng, Y.C. Jean and X.H. Luo, Critical Review of Analytical Chemistry 21 (1989) 209.
[6] P.J. Schultz and K.G. Lynn, Rev. Mod. Phys. 60 (1988) 701.
[7] A. Vehanen, Hyp. Int. 45 (1989) 179.
[8] I.J. Rosenberg, A.H. Weiss and K.F. Canter, Phys. Rev. Lett. 44 (1980) 1139.
[9] A. Weiss, R. Mayer, M. Jibaly, C. Lei, D. Mehl and K.G. Lynn, Phys. Rev. Lett. 61 (1988) 2245.
[10] P.A. Huttunen, J. Mäkinen, D.T. Britton, E. Soininen and A. Vehanen, Phys. Rev. B, in press.
[11] J. van House and A. Rich, Phys. Rev. Lett. 60 (1988) 169.
[12] J. van House and A. Rich, Phys. Rev. Lett. 61 (1988) 488.
[13] E. Tandberg, P.J. Schultz, G.C. Aers and T.E. Jackman, Can. J. Phys. 67 (1989) 275.
[14] *Positron and Positronium Chemistry*, eds. D.M. Schrader and Y.C. Jean, Studies in Physical and Theoretical Chemistry, Vol. 57 (Elsevier, Amsterdam 1988).
[15] *Positron Annihilation*, eds. P.G. Coleman, S.C. Sharma and L.M. Diana (North-Holland, 1982).
[16] *Positron Annihilation*, eds. P.C. Jain, R.M. Singru and K.P. Gopianathan (World Scientific, Singapore, 1985).
[17] *Positron Annihilation*, eds. L. Dorikens-Vanpraet, M. Dorikens and D. Segers (World Scientific, Singapore, 1988).
[18] A. Vehanen, K. Saarinen, P. Hautojärvi and H. Huomo, Phys. Rev. B 35 (1987) 8252.
[19] S. Valkelahti and R.M. Nieminen, Appl. Phys. A 32 (1983) 95 and 35 (1984) 51.
[20] A. Perkins and J.P. Carbotte, Phys. Rev. B 1 (1970) 101.
[21] H. Huomo, A. Vehanen, M.D. Bentzon and P. Hautojärvi, Phys. Rev. B 35 (1987) 8252.
[22] A.P. Mills Jr., in: ref. [4].
[23] A. Dupasquier, in: ref. [4].
[24] A. Vehanen, K.G. Lynn, P.J. Schultz and M. Eldrup, Appl. Phys. A 32 (1983) 163.
[25] R.H. Howell, M.J. Fluss and I.J. Rosenberg, Nucl. Instr. Meth. B 10/11 (1985) 377.
[26] J. Lahtinen, A. Vehanen, H. Huomo, J. Mäkinen, P. Huttunen, K. Rytsölä, M. Bentzon and P. Hautojärvi, Nucl. Instr. Meth. B 17 (1986) 73.
[27] A. Vehanen and J. Mäkinen, Appl. Phys. A 36 (1985) 97.
[28] E. Gramsch, J. Throwe and K.G. Lynn, Appl. Phys. Lett. 51 (1987) 1862.
[29] J. van House and P.W. Zitzewitz, Phys. Rev. A 29 (1984) 96.
[30] K.G. Lynn and A.W. Frieze, in: *Positron Scattering in Gases*, eds. J.W. Humberston and M.C.R. McDowell, NATO ASI Series B, Vol. 107 (Plenum Press, 1983).
[31] A.P. Mills, Jr. and E.M. Gullikson, Appl. Phys. Lett. 49 (1986) 1121.
[32] J. Mäkinen, A. Vehanen, P. Hautojärvi, H. Huomo, J. Lahtinen, R.M. Nieminen and S. Valkealahti, Surf. Sci. 175 (1986) 385.
[33] M.D. Benzton, H. Huomo, A. Vehanen, P. Hautojärvi, J. Lahtinen and M. Hautala, J. Phys. F 17 (1987) 1477.
[34] P.J. Schultz, K.G. Lynn, W.E. Frieze and A. Vehanen, Phys. Rev. B 27 (1983) 6626.
[35] J.G. Ociepa, P.J. Schultz, K. Griffiths and P.R. Norton, Surface Sci. 225 (1990) 281.
[36] P.A. Huttunen, J. Mäkinen and A. Vehanen, Phys. Rev. B 41 (1990) 8062.
[37] P.A. Huttunen and A. Vehanen, Phys. Rev. B, in press.

[38] J. Keinonen, M. Hautala, E. Rauhala, V. Karttunen, A. Kuronen, J. Räisänen, J. Lahtinen, A. Vehanen, E. Punkka and P. Hautojärvi, Phys. Rev. B 37 (1988) 8269.
[39] K.G. Lynn, B. Nielsen and D.O. Welch, Can. J. Phys. 67 (1989) 818.
[40] *Electron Spectroscopy for Surface Analysis*, ed. H. Ibach, Topics in Current Physics, Vol. 4 (Springer-Verlag 1977).
[41] M.N. Read and D.N. Lowy, Surf. Sci. 107 (1981) L313.
[42] A.H. Weiss, I.J. Rosenberg, K.F. Canter, C.B. Duke and A. Paton, Phys. Rev. B 27 (1983) 867.
[43] R. Mayer, C.-S. Zhang, K.G. Lynn, W.E. Frieze, F. Jona and P.M. Marcus, Phys. Rev. B 35 (1987) 3102.
[44] W.E. Frieze, D.W. Gidley and K.G. Lynn, Phys. Rev. B 31 (1985) 5628.
[45] A.P. Mills, Jr. and W.S. Crane, Phys. Rev. B 31 (1985) 3988.
[46] D. Mehl, A.R. Köymen, K.O. Jensen, F. Gotwald and A. Weiss, Phys. Rev. B 41 (1990) 799.
[47] C. Lei, D. Mehl, A.R. Köymen, F. Gotwald, M. Jibaly and A. Weiss, Rev. Sci. Instrum. 60 (1989) 3656.
[48] D.A. Fisher, K.G. Lynn and W.E Frieze, Phys. Rev. Lett. 50 (1983) 1149.
[49] D.A. Fisher, K.G. Lynn and D.W. Gidley, Phys. Rev. B 33 (1986) 4479.
[50] G.R. Brandes, K.F. Canter and A.P. Mills, Jr., Phys. Rev. Lett. 61 (1988) 492.
[51] W.E. Frieze, D.W. Gidley, A. Rich and J. van House, Nucl. Instrum. Meth. A, submitted.
[52] W.E. Frieze, D.W. Gidley and B.D. Wissman, Solid State Comm., submitted.
[53] A.R. Köymen, D.W. Gidley and T.W. Capehart, Phys. Rev. B 35 (1987) 1034.
[54] R.H. Howell, P. Meyer, I.J. Rosenberg and M.J. Fluss, Phys. Rev. Lett. 54 (1985) 1698.
[55] D.M. Chen, S. Berko, K.F. Canter, K.G. Lynn, A.P. Mills Jr., L.O. Roellig, P. Sferlazzo, M. Weinert and R.N. West, Phys. Rev. B 39 (1989) 3966 and references there.
[56] D.M. Chen, Ph.D. Dissertation, City College, New York, 1987.
[57] P. Sferlazzo, S. Berko, K.F. Canter, K.G. Lynn, A.P. Mills Jr., L.O. Roellig, A. Viescas and R.N. West, Phys. Rev. Lett. 60 (1988) 538.
[58] R.H. Howell, I.J. Rosenberg, P. Meyer and M.J. Fluss, Phys. Rev. B 35 (1987) 4555.
[59] D.T. Britton, P.A. Huttunen, J. Mäkinen, E. Soininen and A. Vehanen, Phys. Rev. Lett. 62 (1989) 2413.
[60] Y. Kong, R.M. Nieminen, P.A. Huttunen, A. Vehanen and J. Mäkinen, Europhys. Lett., submitted.
[61] P.A. Huttunen, A. Vehanen and R.M. Nieminen, Phys. Rev. B 40 (1989) 11923.
[62] D.W. Gidley, A.R. Köymen and T.w. Capehart, Phys. Rev. Lett. 49 (1982) 1779.
[63] D.W. Gidley, A.R. Köymen and T.W. Capehart, Phys. Rev. B 37 (1988) 2465.
[64] K.G. Lynn, Phys. Rev. Lett. 44 (1980) 1330.
[65] Y.-C. Chen, K.G. Lynn and B. Nielsen, Phys. Rev. B 37 (1988) 3105.
[66] see f.ex. *Catalyst Characterization Science*, eds. M.L. Deviney and J.L. Gland, ACS Symposium Series 288 (Am. Chem. Soc., 1985).
[67] K. Venkateswaran, K.L. Cheng and Y.C. Jean, J. Phys. Chem. 88 (1984) 2465.
[68] Y. Ito and T. Takano, Appl. Phys. A 45 (1988) 193.
[69] Y. Ito, M. Hirose and Y. Tabata, Appl. Phys. A 50 (1990) 39.
[70] H. Nakanishi and Y. Ujihira, J. Phys. Chem. 86 (1982) 4446.
[71] M. Debowska, A. Baranowski, K. Jerie and B. Sulikowski, in: ref. [17].
[72] M. Debowska, J. Ch. Abbé and G. Duplatre, Phys. Stat. Sol. B 146 (1988) 91.
[73] J. Lahtinen, K. Fallström, P. Kuusisto, A. Vehanen and P. Hautojärvi, to be published.
[74] X.L. Lou, K.L. Cheng and Y.C. Jean, in: ref. [16].
[75] I.Ya. Dekhtyar, R.G. Fedchenko and Y.M. Sagov, Khim. Fiz. 8 (1982) 1101-4 and 11 (1983) 1573-6 (in Russian).
[76] O.E. Mogensen, M. Eldrup, S. Mørup, J.W. Ørnbo and H. Topsøe, in: ref. [16].
[77] A.D. Mokrushin, E.P. Prokopev and A.D. Tsyganov, Kinet. Catal. (USSR) 11 (1970) 666.

[78] K. Venkateswaran, K.L. Cheng and Y.C. Jean, J. Phys. Chem. 89 (1985) 3001.
[79] K. Venkateswaran, K.L. Cheng and Y.C. Jean, Chem. Phys. Lett. 126 (1986) 33.
[80] K.P. Aref'ev, P.V. Kuznetsov, V.S. Mikhalenkov, S.V. Kholodkevich and I. Yuli-Kauppila, Sov. Phys. Solid State 26 (1984) 237.
[81] Y.C. Jean, C. Yu and D-M. Zhou, Phys. Rev. B 32 (1985) 4313.
[82] N. Hozhabri, S.C. Sharma and S.J. Wang, in: ref [17].
[83] S.J. Wang and Y.J. Jean, Phys. Rev. B 37 (1988) 4869.
[84] S.J. Wang, D.-M. Zhou and Y.J. Jean, Chem. Phys. 129 (1989) 503.